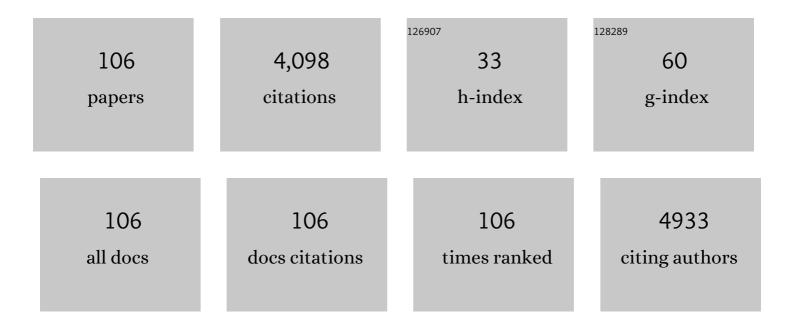
List of Publications by Year in descending order

Source: https://exaly.com/author-pdf/2023802/publications.pdf Version: 2024-02-01



YUZHENC GUO

#	Article	IF	CITATIONS
1	Theoretical Insights into the Mechanism of Selective Nitrateâ€toâ€Ammonia Electroreduction on Singleâ€Atom Catalysts. Advanced Functional Materials, 2021, 31, 2008533.	14.9	240
2	Unraveling the Origin of Sulfurâ€Doped Feâ€Nâ€C Singleâ€Atom Catalyst for Enhanced Oxygen Reduction Activity: Effect of Iron Spinâ€State Tuning. Angewandte Chemie - International Edition, 2021, 60, 25404-25410.	13.8	177
3	A durable and pH-universal self-standing MoC–Mo2C heterojunction electrode for efficient hydrogen evolution reaction. Nature Communications, 2021, 12, 6776.	12.8	169
4	Computational Screening Single-Atom Catalysts Supported on g-CN for N ₂ Reduction: High Activity and Selectivity. ACS Sustainable Chemistry and Engineering, 2020, 8, 13749-13758.	6.7	167
5	Origin of the high work function and high conductivity of MoO3. Applied Physics Letters, 2014, 105, .	3.3	161
6	Band engineering in transition metal dichalcogenides: Stacked versus lateral heterostructures. Applied Physics Letters, 2016, 108, .	3.3	151
7	Revealing the oxygen reduction reaction activity origin of single atoms supported on g-C ₃ N ₄ monolayers: a first-principles study. Journal of Materials Chemistry A, 2020, 8, 6555-6563.	10.3	140
8	Calculation of TiO ₂ Surface and Subsurface Oxygen Vacancy by the Screened Exchange Functional. Journal of Physical Chemistry C, 2015, 119, 18160-18166.	3.1	136
9	Single-Atom Rhodium on Defective g-C ₃ N ₄ : A Promising Bifunctional Oxygen Electrocatalyst. ACS Sustainable Chemistry and Engineering, 2021, 9, 3590-3599.	6.7	136
10	3D Behavior of Schottky Barriers of 2D Transition-Metal Dichalcogenides. ACS Applied Materials & Interfaces, 2015, 7, 25709-25715.	8.0	134
11	Impact of oxygen exchange reaction at the ohmic interface in Ta ₂ O ₅ -based ReRAM devices. Nanoscale, 2016, 8, 17774-17781.	5.6	116
12	Defect passivation of transition metal dichalcogenides via a charge transfer van der Waals interface. Science Advances, 2017, 3, e1701661.	10.3	95
13	Materials selection for oxide-based resistive random access memories. Applied Physics Letters, 2014, 105, .	3.3	92
14	A Feasible Strategy for Identifying Singleâ€Atom Catalysts Toward Electrochemical NOâ€ŧoâ€NH ₃ Conversion. Small, 2021, 17, e2102396.	10.0	89
15	Electronic and magnetic properties of Ti ₂ O ₃ , Cr ₂ O ₃ , and Fe ₂ O ₃ calculated by the screened exchange hybrid density functional. Journal of Physics Condensed Matter, 2012, 24, 325504.	1.8	82
16	A New Opportunity for 2D van der Waals Heterostructures: Making Steepâ€ S lope Transistors. Advanced Materials, 2020, 32, e1906000.	21.0	82
17	Machine-Learning-Accelerated Catalytic Activity Predictions of Transition Metal Phthalocyanine Dual-Metal-Site Catalysts for CO ₂ Reduction. Journal of Physical Chemistry Letters, 2021, 12, 6111-6118.	4.6	80
18	Blowing Iron Chalcogenides into Two-Dimensional Flaky Hybrids with Superior Cyclability and Rate Capability for Potassium-Ion Batteries. ACS Nano, 2021, 15, 2506-2519.	14.6	79

#	Article	IF	CITATIONS
19	Localized Tail States and Electron Mobility in Amorphous ZnON Thin Film Transistors. Scientific Reports, 2015, 5, 13467.	3.3	70
20	Selective Passivation of GeO ₂ /Ge Interface Defects in Atomic Layer Deposited High- <i>k</i> MOS Structures. ACS Applied Materials & Interfaces, 2015, 7, 20499-20506.	8.0	66
21	Iron Selenide Microcapsules as Universal Conversionâ€Typed Anodes for Alkali Metalâ€Ion Batteries. Small, 2021, 17, e2005745.	10.0	66
22	Light induced instability mechanism in amorphous InGaZn oxide semiconductors. Applied Physics Letters, 2014, 104, .	3.3	60
23	Photonic-plasmonic hybrid single-molecule nanosensor measures the effect of fluorescent labels on DNA-protein dynamics. Science Advances, 2017, 3, e1602991.	10.3	57
24	Vacancy and Doping States in Monolayer and bulk Black Phosphorus. Scientific Reports, 2015, 5, 14165.	3.3	55
25	Phase boundary engineering of metal-organic-framework-derived carbonaceous nickel selenides for sodium-ion batteries. Nano Research, 2020, 13, 2289-2298.	10.4	51
26	Theoretical study on the photocatalytic properties of 2D InX(X = S, Se)/transition metal disulfide (MoS ₂ and WS ₂) van der Waals heterostructures. Nanoscale, 2020, 12, 20025-20032.	5.6	49
27	Oxygen vacancy defects in Ta2O5 showing long-range atomic re-arrangements. Applied Physics Letters, 2014, 104, .	3.3	42
28	Two-Dimensional Gallium Oxide Monolayer for Gas-Sensing Application. Journal of Physical Chemistry Letters, 2021, 12, 5813-5820.	4.6	41
29	An aqueous zincâ€ion battery working at â^50°C enabled by lowâ€concentration perchlorateâ€based chaotropic salt electrolyte. EcoMat, 2022, 4, .	11.9	40
30	Efficient Transfer Doping of Carbon Nanotube Forests by MoO ₃ . ACS Nano, 2015, 9, 10422-10430.	14.6	39
31	Band structure, band offsets, substitutional doping, and Schottky barriers of bulk and monolayer InSe. Physical Review Materials, 2017, 1, .	2.4	39
32	Unraveling the Origin of Sulfurâ€Doped Feâ€Nâ€C Singleâ€Atom Catalyst for Enhanced Oxygen Reduction Activity: Effect of Iron Spinâ€State Tuning. Angewandte Chemie, 2021, 133, 25608-25614.	2.0	38
33	Chemical bonding and band alignment at X2O3/GaN (X = Al, Sc) interfaces. Applied Physics Letters, 2019 114, .	9, 3.3	36
34	Tuning Ni dopant concentration to enable co-deposited superhydrophilic self-standing Mo2C electrode for high-efficient hydrogen evolution reaction. Applied Catalysis B: Environmental, 2022, 307, 121201.	20.2	36
35	Theoretical investigation on graphene-supported single-atom catalysts for electrochemical CO ₂ reduction. Catalysis Science and Technology, 2020, 10, 8465-8472.	4.1	35
36	Revealing the oxygen Reduction/Evolution reaction activity origin of Carbon-Nitride-Related Single-Atom catalysts: Quantum chemistry in artificial intelligence. Chemical Engineering Journal, 2022, 440, 135946.	12.7	35

#	Article	IF	CITATIONS
37	Interface Engineering for Atomic Layer Deposited Alumina Gate Dielectric on SiGe Substrates. ACS Applied Materials & Interfaces, 2016, 8, 19110-19118.	8.0	34
38	Anisotropic Transport Property of Antimonene MOSFETs. ACS Applied Materials & Interfaces, 2020, 12, 22378-22386.	8.0	30
39	Tellurium Nanowire Gate-All-Around MOSFETs for Sub-5 nm Applications. ACS Applied Materials & Interfaces, 2021, 13, 3387-3396.	8.0	30
40	Comparison of oxygen vacancy defects in crystalline and amorphous Ta2O5. Microelectronic Engineering, 2015, 147, 254-259.	2.4	25
41	Graphene–Organic Two-Dimensional Charge-Transfer Complexes: Intermolecular Electronic Transitions and Broadband Near-Infrared Photoresponse. Journal of Physical Chemistry C, 2018, 122, 7551-7556.	3.1	25
42	The metal–insulator phase change in vanadium dioxide and its applications. Journal of Applied Physics, 2021, 129, .	2.5	25
43	A new opportunity for the emerging tellurium semiconductor: making resistive switching devices. Nature Communications, 2021, 12, 6081.	12.8	25
44	Electrical conduction of carbon nanotube forests through sub-nanometric films of alumina. Applied Physics Letters, 2013, 102, .	3.3	24
45	Calculation of metallic and insulating phases of V2O3 by hybrid density functionals. Journal of Chemical Physics, 2014, 140, 054702.	3.0	24
46	The Electrophilicity of Surface Carbon Species in the Redox Reactions of CuOâ€CeO ₂ Catalysts. Angewandte Chemie - International Edition, 2021, 60, 14420-14428.	13.8	24
47	Chemical trends of defects at HfO2:GaAs and Al2O3:GaAs/InAs/InP/GaSb interfaces. Journal of Applied Physics, 2013, 113, .	2.5	22
48	Band edge states, intrinsic defects, and dopants in monolayer HfS2 and SnS2. Applied Physics Letters, 2018, 112, .	3.3	22
49	Enhanced electrochemical oxygen evolution reaction activity on natural single-atom catalysts transition metal phthalocyanines: the substrate effect. Catalysis Science and Technology, 2020, 10, 8339-8346.	4.1	22
50	An Atomically Thin Air‣table Narrowâ€Gap Semiconductor Cr ₂ S ₃ for Broadband Photodetection with High Responsivity. Advanced Electronic Materials, 2021, 7, 2000962.	5.1	22
51	Oxygen vacancies and hydrogen in amorphous In-Ga-Zn-O and ZnO. Physical Review Materials, 2018, 2, .	2.4	21
52	Two-dimensional metal–organic frameworks as efficient electrocatalysts for bifunctional oxygen evolution/reduction reactions. Journal of Materials Chemistry A, 2022, 10, 13005-13012.	10.3	21
53	A fast transfer-free synthesis of high-quality monolayer graphene on insulating substrates by a simple rapid thermal treatment. Nanoscale, 2016, 8, 2594-2600.	5.6	20
54	Hydrogen and the Light-Induced Bias Instability Mechanism in Amorphous Oxide Semiconductors. Scientific Reports, 2017, 7, 16858.	3.3	19

#	Article	IF	CITATIONS
55	Carbon cluster formation and mobility degradation in 4H-SiC MOSFETs. Applied Physics Letters, 2021, 118, .	3.3	18
56	Reduced Fermi Level Pinning at Physisorptive Sites of Moire-MoS ₂ /Metal Schottky Barriers. ACS Applied Materials & Interfaces, 2022, 14, 11903-11909.	8.0	17
57	Identifying TM-N4 active sites for selective CO2-to-CH4 conversion: A computational study. Applied Surface Science, 2022, 582, 152470.	6.1	16
58	(In <i>_x</i> Ga _{1â^'} <i>_x</i>) ₂ O ₃ Thin Film Based Solarâ€Blind Deep UV Photodetectors with Ultraâ€High Detectivity and On/Off Current Ratio. Advanced Optical Materials, 2022, 10, .	7.3	16
59	Impact of the interface vacancy on Schottky barrier height for Au/AlN polar interfaces. Applied Surface Science, 2020, 505, 144650.	6.1	15
60	Face Dependence of Schottky Barriers Heights of Silicides and Germanides on Si and Ge. Scientific Reports, 2017, 7, 16669.	3.3	14
61	Extending the metal-induced gap state model of Schottky barriers. Journal of Vacuum Science and Technology B:Nanotechnology and Microelectronics, 2020, 38, .	1.2	14
62	Schottky barrier heights of defect-free metal/ZnO, CdO, MgO, and SrO interfaces. Journal of Applied Physics, 2021, 129, .	2.5	14
63	Self-Poisoning by C ₂ Products in CO ₂ Photoreduction Using a Phosphorus-Doped Carbon Nitride with Nitrogen Vacancies. ACS Sustainable Chemistry and Engineering, 2022, 10, 5758-5769.	6.7	14
64	Impact of Coordination Environment on Single-Atom-Embedded C ₃ N for Oxygen Electrocatalysis. ACS Sustainable Chemistry and Engineering, 2022, 10, 7692-7701.	6.7	14
65	Chemical trends of Schottky barrier behavior on monolayer hexagonal B, Al, and Ga nitrides. Journal of Applied Physics, 2016, 120, .	2.5	13
66	Schottky barrier height at metal/ZnO interface: A first-principles study. Microelectronic Engineering, 2019, 216, 111056.	2.4	13
67	Structural changes during the switching transition of chalcogenide selector devices. Applied Physics Letters, 2019, 115, .	3.3	13
68	Tuning the high-κ oxide (HfO2, ZrO2)/4H-SiC interface properties with a SiO2 interlayer for power device applications. Applied Surface Science, 2020, 527, 146843.	6.1	13
69	Defects and Passivation Mechanism of the Suboxide Layers at SiOâ,,/4H-SiC (0001) Interface: A First-Principles Calculation. IEEE Transactions on Electron Devices, 2021, 68, 288-293.	3.0	13
70	A density-functional-theory-based and machine-learning-accelerated hybrid method for intricate system catalysis. Materials Reports Energy, 2021, 1, 100046.	3.2	13
71	Atomic structure and band alignment at Al2O3/GaN, Sc2O3/GaN and La2O3/GaN interfaces: A first-principles study. Microelectronic Engineering, 2019, 216, 111039.	2.4	12
72	Controllable Thermal Oxidation and Photoluminescence Enhancement in Quasi-1D van der Waals ZrS ₃ Flakes. ACS Applied Electronic Materials, 2020, 2, 3756-3764.	4.3	12

#	Article	IF	CITATIONS
73	Modelling the enthalpy change and transition temperature dependence of the metal–insulator transition in pure and doped vanadium dioxide. Physical Chemistry Chemical Physics, 2020, 22, 13474-13478.	2.8	12
74	p-Type Semiconduction in Oxides with Cation Lone Pairs. Chemistry of Materials, 2022, 34, 643-651.	6.7	12
75	Origin of Weaker Fermi Level Pinning and Localized Interface States at Metal Silicide Schottky Barriers. Journal of Physical Chemistry C, 2020, 124, 19698-19703.	3.1	11
76	Electronic structure of metallic and insulating phases of vanadium dioxide and its oxide alloys. Physical Review Materials, 2019, 3, .	2.4	11
77	An all two-dimensional vertical heterostructure graphene/CuInP ₂ S ₆ /MoS ₂ for negative capacitance field effect transistor. Nanotechnology, 2022, 33, 125703.	2.6	11
78	The effects of screening length in the non-local screened-exchange functional. Journal of Physics Condensed Matter, 2015, 27, 025501.	1.8	10
79	Ab initio calculations of materials selection of oxides for resistive random access memories. Microelectronic Engineering, 2015, 147, 339-343.	2.4	10
80	Charge transfer doping of graphene without degrading carrier mobility. Journal of Applied Physics, 2017, 121, .	2.5	10
81	Electronic properties and tunability of the hexagonal SiGe alloys. Applied Physics Letters, 2021, 118, .	3.3	10
82	Electronic structure of amorphous copper iodide: A <mml:math xmlns:mml="http://www.w3.org/1998/Math/MathML"><mml:mi>p</mml:mi> -type transparent semiconductor. Physical Review Materials, 2020, 4, .</mml:math 	2.4	10
83	Moiré flat bands in twisted 2D hexagonal vdW materials. 2D Materials, 2022, 9, 014005.	4.4	10
84	Strain-promoted conductive metal-benzenhexathiolate frameworks for overall water splitting. Journal of Colloid and Interface Science, 2022, 624, 160-167.	9.4	10
85	Band Structure, Band Offsets, and Intrinsic Defect Properties of Few-Layer Arsenic and Antimony. Journal of Physical Chemistry C, 2020, 124, 7441-7448.	3.1	9
86	Hybrid band offset calculation for heterojunction interfaces between disparate semiconductors. Applied Physics Letters, 2020, 116, .	3.3	9
87	Tunable contacts and device performances in graphene/group-III monochalcogenides MX (M = In, Ga;)	Tj ETQq1	1 0. <mark>7</mark> 84314 g
88	Negative Differential Resistance Effect in "Cold―Metal Heterostructure Diodes. IEEE Electron Device Letters, 2022, 43, 498-501.	3.9	8
89	Electronic properties of CaF2 bulk and interfaces. Journal of Applied Physics, 2022, 131, .	2.5	8
90	Phase dependence of Schottky barrier heights for Ge–Sb–Te and related phase-change materials. Journal of Applied Physics, 2020, 127, .	2.5	7

#	Article	IF	CITATIONS
91	Role of the third metal oxide in In–Ca–Zn–O4 amorphous oxide semiconductors: Alternatives to gallium. Journal of Applied Physics, 2020, 128, 215704.	2.5	6
92	Termination-dependence of Fermi level pinning at rare-earth arsenide/GaAs interfaces. Applied Physics Letters, 2020, 116, .	3.3	6
93	<i>Ab Initio</i> Study of Hexagonal Boron Nitride as the Tunnel Barrier in Magnetic Tunnel Junctions. ACS Applied Materials & amp; Interfaces, 2021, 13, 47226-47235.	8.0	6
94	Computation-guided design and preparation of durable and efficient WC-Mo2C heterojunction for hydrogen evolution reaction. Cell Reports Physical Science, 2022, 3, 100784.	5.6	6
95	Highâ€Throughput Electronic Structures and Ferroelectric Interfaces of HfO 2 by GGA+ U (d,p) Calculations. Physica Status Solidi - Rapid Research Letters, 2021, 15, 2100295.	2.4	5
96	Controllable High-Performance Memristors Based on 2D Fe2GeTe3 Oxide for Biological Synapse Imitation. Nanotechnology, 2021, 32, .	2.6	4
97	Impact of carbon–carbon defects at the SiO ₂ /4H-SiC (0001) interface: a first-principles calculation. Journal Physics D: Applied Physics, 2022, 55, 025109.	2.8	4
98	Machineâ€learningâ€based interatomic potentials for advanced manufacturing. International Journal of Mechanical System Dynamics, 2021, 1, 159-172.	2.8	4
99	A Marr's Threeâ€Level Analytical Framework for Neuromorphic Electronic Systems. Advanced Intelligent Systems, 2021, 3, 2100054.	6.1	3
100	Effect of Phase Transition on Optical Properties and Photovoltaic Performance in Cesium Lead Bromine Perovskite: A Theoretical Study. Journal of Physical Chemistry C, 2019, 123, 20764-20768.	3.1	2
101	Band alignment calculation of dielectric films on VO2. Microelectronic Engineering, 2019, 216, 111057.	2.4	2
102	The Electrophilicity of Surface Carbon Species in the Redox Reactions of CuO eO 2 Catalysts. Angewandte Chemie, 2021, 133, 14541-14549.	2.0	2
103	Frontispiece: The Electrophilicity of Surface Carbon Species in the Redox Reactions of CuO eO ₂ Catalysts. Angewandte Chemie - International Edition, 2021, 60, .	13.8	1
104	Large piezoelectricity response in Li and Ti (or Zr) co-alloyed w-AlN. Journal of Applied Physics, 2022, 131, .	2.5	1
105	Oxide defects and reliability of high K/Ge and IIIâ \in V based gate stacks. , 2015, , .		0
106	Frontispiz: The Electrophilicity of Surface Carbon Species in the Redox Reactions of CuO eO ₂ Catalysts. Angewandte Chemie, 2021, 133, .	2.0	0